Lightning Current Distribution to Ground at a Power Line Tower Carrying a Radio Base Station

Leonid Grcev, *Senior Member, IEEE*, A. (Lex) P. J. van Deursen, *Senior Member, IEEE*, and J. B. M. van Waes

***Abstract*—Radio base stations are often mounted on towers of power transmission lines. They are usually powered from the low-voltage network through an isolating transformer, to separate the high- and low-voltage networks. The isolating transformer ensures security at customers' premises in the case of nearby power faults and particularly in case of lightning striking, which is a frequent cause of flashover of the high-voltage insulators and a subsequent phase-to-ground fault. To optimize such protection, a better understanding of the current distribution to the ground in the initial phase of the lightning striking is required. This paper presents a computer simulation method and its results for the lightning current distribution between the sky wires, grounding systems, and power cable network. What is of special concern is the part of the lightning current that might be led into the metal-shielded distribution cable network. A rigorous electromagnetic modeling approach was applied for the analysis of the grounding effects in a network of coated and uncoated low- and medium-voltage cables. The analysis was then applied to a practical case.**

***Index Terms*—Grounding, lightning, power cables, power system lightning effects, radio base stations.**

I. Introduction

RADIO base stations are often mounted on towers of power transmission lines. Lightning striking the line may induce flashover of the high-voltage (HV) insulators and a subsequent phase-to-ground fault (see, for example, [1] and [2]). The resulting currents usually distribute to the ground through the tower grounding and over the sky wires. However, if the radio base station is powered by a low-voltage (LV) cable, a fraction of the power frequency fault current might flow through the LV cable toward the medium-voltage/low-voltage (MV/LV) transformer station (TS) [3] (Fig. 1). This may cause dangerous voltages in customers' premises served by the same TS. An electromagnetic transients program (EMTP) [4] calculation showed that values larger than 1.5 kV can occur in an actual HV line on a dry-sand soil [5, page 45]. Appropriate measures could guarantee safety, for instance, by installing an isolating transformer to separate the faulted HV and the LV network. Special attention is paid to the protection of the isolation transformer, which is usually taken care of by suitable overvoltage arrestors. Such arrestors should withstand the power frequency overvoltage between the tower grounding and the rest of the LV network, but could pass on some part of the lightning's impulse current. Different options for protection schemes depend on practices in different countries [6]–[10]. To analyze the protection measures, and especially the lightning current stress for the overvoltage arrestor that protects the isolating transformer, better knowledge of the lightning current distribution is required.

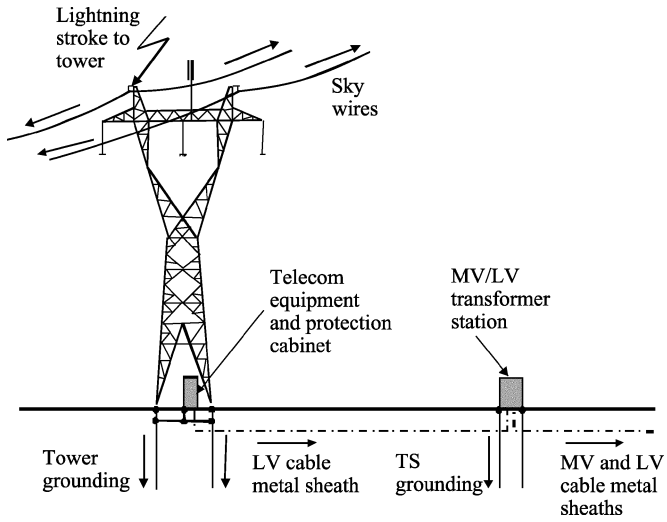

Fig. 1. Lightning strokes a tower with a radio base station (arrows point to the possible lightning current distribution).

Previous work [6], [7] discussed protection measures but concerned only power frequency. Reference [8] estimated overvoltages due to lightning impulse currents utilizing a simple circuit model of the tower grounding. None of these works [6]–[8] included the effects of the LV cable metal sheaths. The most detailed experimental and theoretical analysis of this problem, which considered the MV/LV cable network, was performed in [5], [9], and [10], however, only for power frequency.

This paper extends the analysis to high frequencies and transients related to lightning. The emphasis is on the modeling of the complex buried conductor network consisting of connected grounding electrode arrangements and uncoated and/or coated power cables. Such an analysis provides insight into trends in the high-frequency and transient current distribution to ground at the tower with the radio base station subjected to a lightning bolt (Fig. 1). The distribution of transient current between the grounding system of the tower and the metallic shields of the MV/LV cable network is of particular interest. This distribution causes lightning current stress for the overvoltage arrestor that

Manuscript received August 26, 2003; revised June 13, 2004.

L. Grcev is with the Department of Electrical Engineering, Eindhoven University of Technology, 5600 MB Eindhoven, The Netherlands, on leave from the Faculty of Electrical Engineering, Sts. Cyril and Methodius University, 1000 Skopje, Macedonia (e-mail: leonid.grcev@ieee.org).

A. P. J. van Deursen is with the Department of Electrical Engineering, Eindhoven University of Technology, 5600 MB Eindhoven, The Netherlands (e-mail: a.p.j.v.deursen@tue.nl).

J. B. M. van Waes was with the Department of Electrical Engineering, Eindhoven University of Technology, 5600 MB Eindhoven, The Netherlands. He is now with Holland Railconsult, Utrecht, The Netherlands (e-mail: jvanwaes@hr.nl).

Digital Object Identifier 10.1109/TEMC.2004.842097

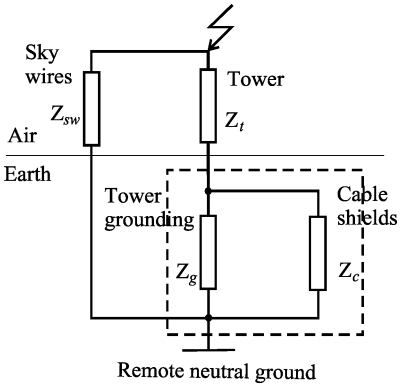

Fig. 2. Circuit representation of the tower struck by lightning.

protects the isolating transformer. The modeling was applied to the same situation in a rural area where the experiments at power frequency had been performed before [5], [9], [10].

The primary goal was to provide a model for the high-frequency grounding effects in a network of buried distribution coated and/or uncoated cables that would be general enough to enable an estimation of the lightning current distribution in similar practical situations. Additionally, such a model was aimed to be applicable in other similar simulation studies, for example, related to grounding in rural and urban areas [11], lightning protection [12], [13], and emerging power line communication technology [14].

II. Method of Analysis

The analysis was carried out in the frequency domain up to 1 MHz, and transient responses were subsequently computed by Fourier transform techniques. Different approaches were applied to model the above and below-ground parts of the systems. The above-ground parts (sky wires with connected towers) could be modeled by a standard simplified circuit approach, while below-ground parts (grounding systems and connected cable network) could be modeled more rigorously using an electromagnetic approach. One reason for this is that the wavelength in air is 300 m for the highest frequency of interest (1 MHz), which allows for the usual circuit-based modeling. However, the wavelength for the same frequency in the soil considered (resistivity 100 Ωm and relative permittivity 10; cf.Section VI) is 22 m, which restricts the use of circuit-based models for large and complex conductor networks such as those modeled in this study [15]. The mutual influences between above- and below-ground parts were neglected. The argument for this approximation is given in Section VIII and is related to the good agreement between simulation and experimental results at low frequencies and to the large difference in impedances to the ground of above and below-ground structures at higher frequencies. A simple circuit representation of the tower struck by lightning is illustrated in Fig. 2 (the broken-line box in Fig. 2 designates coupled impedances; please see remarks in Section IX-B). To determine the current distribution, impedances to the ground of different current paths are required. For below-ground parts, the coupled impedances of the tower grounding and the cable shields, and the current distribution between them, are determined directly from the electromagnetic approach.

The modeling is applied to an existing case [5], [10] for which an analysis of the influence of several parameters is performed, such as the soil conductivity, the quality of the sky wire conductors, and location of the lightning bolt (on the tower or on the sky wires near the tower). The influence of a few typical lightning-current wave shapes was analyzed as well. The results were compared with the available measurements at power frequency.

Nonlinear phenomena related to high current soil ionization and corona at conductors were neglected in the analysis. One justification for this is that, since the main interest was in the current in the power cables, and soil ionization improves the tower grounding performance, this approximation is on the "safe" side (please see additional comments in Section X). The justification for the latter is mentioned in Section IX-C and is related to the dominant influence of the self-impedance of the sky wire conductors on the impedance to the ground. It is worth noting that the inclusion of nonlinear phenomena in the applied frequency-domain method would cause unjustified complications.

III. Modeling of the Grounding System

The electromagnetic model [16] was applied for the frequency and transient three-dimensional (3-D) analysis of complex networks of buried conductors. This model is based on the well-known thin-wire, moment-method antenna model by Richmond [17]. The full details of implementation and validation by comparison with experimental data are available elsewhere [16], [18]. The following briefly summarizes the extensions and modifications of the antenna model that were necessary to use it for grounding systems' analysis.

A computer code (in FORTRAN) is available [19] for the antenna model [17], and the modified code is available online [20] as well. This model is aimed at analysis in the frequency domain of a network of connected or disconnected thin-wire antennas and scatterers arbitrarily oriented in an isotropic, linear, and homogeneous ambient medium. The medium may be conductive, and the code is capable of analyzing thin-wire antennas buried in unbounded soil without taking into account the influence of the air–earth interface. The thin wires may be in direct contact with the soil or insulated by a dielectric coating. Either a voltage generator or an incident wave may energize the thin-wire network.

A. Computations at Low Frequencies

The code [19] is suitable for analysis in megahertz and higher frequency ranges of usual interest in antenna analysis, but grounding studies at lower frequencies (for example, in the kilohertz range) are also of interest. A simple modification by converting the FORTRAN code to DOUBLE PRECISION enables computations at low frequencies. This has proved to be sufficient by numerous comparisons with measurements and standard software for the 50/60-Hz analysis of grounding systems; see, for example, [21].

B. Influence of the Air–Earth Interface

The first approximation that takes into account the influence of the air–earth interface is modified image theory [16]. We briefly consider the application of this approximation for the

range of parameters studied in this paper using the following argument. The wavenumbers in the earth and air are as follows:

$$\begin{aligned} k_e &= \omega\sqrt{\mu_0 \underline{\varepsilon}_e} \\ k_0 &= \omega\sqrt{\mu_0 \varepsilon_0} \\ \underline{\varepsilon}_e &= \varepsilon_e - \frac{j\sigma_e}{\omega} \end{aligned} \tag{1}$$

where σ_e and ε_e are the conductivity and permittivity of the earth, respectively, and ε_0 and μ_0 are the permittivity and permeability of the air, respectively. Here ω is the angular frequency and $j = \sqrt{-1}$. Grounding electrodes are located at a small distance from the air-earth interface (mostly $h \approx 1$ m) and, since $|k_e h| \ll 1$, they are strongly affected by the air–earth interface [22]. In the range of parameters studied in this paper, i.e., for frequencies up to 1 MHz, a conductivity of earth from 0.01 to 0.001 S/m and a relative permittivity of earth 10, the reflection coefficient seen by the grounding electrodes $(k_e - k_0)/(k_e + k_0)$ is in the range of $0.90 \div 1$. This means that the reflected electric and magnetic fields from the air–earth interface may be approximated by a grounding electrode image in air with the current in phase with the original one [22].

This approximation is also validated by the comparison with experimental data in [16] for the range of parameters used.

C. Computation of Impedance to the Ground

The grounding systems are usually described by a circuit property: impedance to remote neutral ground. This is equivalent to impedance between terminals of an ideal current source: one at the grounding system and the other at the remote ground, which is theoretically infinitely distant. This is different from antenna source models, which are usually defined between two close terminals, which are theoretically infinitely close.

The definition of the impedance to the ground is facilitated here by the introduction of a current source model capable of injecting current into the grounding system. The following briefly describes such a shunt current source model.

In the piecewise sinusoidal Galerkin method [17], the wire is divided into fictitious segments [Fig. 3(a)], and the current along the wire is represented by samples at the segments' junction points [I_m in Fig. 3(b)]. Current sample I_m at each junction point determines the distributions of current along the neighboring segments, which are approximated by sinusoidal functions along segments with zero current at the segments' ends. Such current distributions at any two neighboring segments form the so-called "sinusoidal dipoles." The overall current distribution along the antenna is approximated by a superposition of overlapped "sinusoidal dipoles." The longitudinal current $I(\ell)$ at point ℓ is then approximated along the conductors' network by a linear combination of M expansion functions $F_m(\ell)$ [see Fig. 3(b)] as follows:

$$\begin{aligned} I(\ell) &= \sum_{m=1}^{M} I_m F_m(\ell) \\ F_m(\ell) &= \frac{\sinh\left[jk_e(\ell - \ell_m)\right]}{\sinh(jk_e d)} \end{aligned} \tag{2}$$

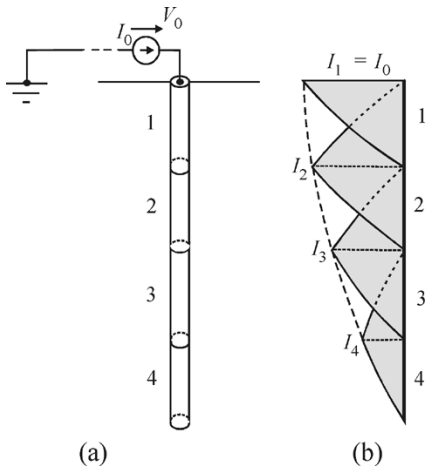

Fig. 3. (a) Grounding electrode represented by four segments. (b) Approximation of current distribution along the electrode.

Here d denotes the length of the segment, and ℓ_m denotes the junction point. It should be noted that the time variation $\exp(j\omega t)$ is suppressed.

Fig. 3 illustrates a straight, vertical, thin grounding electrode with an ideal current source connected between the top of the electrode and the remote "neutral" earth. The influence of the current source leads is neglected. (It should be noted that the choice of a simple straight conductor in Fig. 3 is only for illustration; the model is applicable to networks of connected and/or disconnected segments in an arbitrary orientation.) The current at the top of the grounding electrode is equal to the current source I_0 and is represented by an additional "'sinusoidal monopole" with a current distribution defined by a current sample at the top and sinusoidal distribution along the first segment. The unknown current samples along the antenna may be evaluated by applying the well-known moment methods [17]. For the four-segment example in Fig. 3, if the current source I_0 is used, the following matrix equations lead to the solution for the current distribution I_n:

$$\begin{bmatrix} 1 & 0 & 0 & 0 \\ z_{21} & z_{22} & z_{23} & z_{24} \\ z_{31} & z_{32} & z_{33} & z_{34} \\ z_{41} & z_{42} & z_{43} & z_{44} \end{bmatrix} \cdot \begin{bmatrix} I_1 \\ I_2 \\ I_3 \\ I_4 \end{bmatrix} = \begin{bmatrix} I_0 \\ 0 \\ 0 \\ 0 \end{bmatrix}. \tag{3}$$

Elements z_{mn} of the matrix are related to mutual electromagnetic interactions between sinusoidal dipoles (or monopoles) m and n. More details of the implementation are available elsewhere [16], [18].

The voltage V_0 between the feed point and remote ground (Fig. 3) enables us to define the impedance to the ground

$$Z = \frac{V_0}{I_0}. \tag{4}$$

It is worth noting that the voltage V_0 at high frequencies is path-dependent and may be determined by integration of the electric field along the path of the measuring circuit [16].

IV. Modeling of the Distribution Cable Network

The method described in Section III has been extended to the modeling of high-frequency and transient grounding effects

in a distribution cable network. The grounding effects of uncoated and coated metallic sheathed distribution cables at an industrial frequency have been studied in detail, for example, in [23]–[25]. However, analysis of the grounding effects of a network of coated and uncoated distribution cables at high frequencies and transients has not been performed so far.

Uncoated cables, such as paper-insulated lead-sheathed cables (PILCs), are no longer manufactured in many countries, but many of them still are in operation. The steel armor and the lead sheath of such cables usually come into direct contact with the soil after a period of use. Such cables then behave as extended ground electrodes conducting a considerable portion of the ground fault currents. This usually improves the performance of the connected grounding systems and reduces the associated voltages to the ground. On the other hand, cross-linked polyethylene (XLPE) or polyethylene (PE) insulated polyvinyl chloride (PVC) coated cables are widely used in today's distribution networks. Their metallic shields are insulated from the soil but might be bonded to the grounding systems of the source and/or consumers' transformer stations all along the cables.

The treatment of coated and uncoated arbitrarily configured wires with finite conductivity in a conducting medium has already been built into the method [17], [19]. The thin dielectric layer coated on the wire surface can be modeled by a rigorous approach with equivalent volume polarization currents within the dielectric [27]. Finite conductivity of the wires is taken into account via a concept of a surface impedance [16], [17]. Extending this concept, the code can be applied to the modeling of metal-sheathed distribution cables. Coated cables usually have a single-layer metallic sheath, while uncoated PILC cables have a lead sheath and steel armor that may be approximated by one- and two-layer tubular conductors, respectively [4]. The surface z_s and transfer z_t impedances of a tubular conductor may be computed as follows [4]:

$$\begin{aligned} z_{sk} &= \frac{m_k}{2\pi r_k \sigma_{2k} D_k}\left[I_0(mr_k)K_1(mq_k) + K_0(mr_k)I_1(mq_k)\right] \\ z_{tk} &= \frac{1}{2\pi r_k q_k \sigma_k D_k} \\ D_k &= I_1(mr_k)K_1(mq_k) - I_1(mq_k)K_1(mr_k) \\ m_k &= \sqrt{j\omega\mu_k\sigma_k} \end{aligned} \tag{5}$$

where subscript $_k$ denotes the conductor layer, r_k and q_k are the outside and inside radius, respectively, and σ_k and μ_k are the conductivity and permeability of the kth conductor layer. Here, also, I_0, I_1, K_0, and K_1 are modified Bessel functions [28]. Surface impedances of the one-layer sheath Z_{s1} and the two-layer sheath Z_{s2}, respectively, are [29]

$$\begin{aligned} Z_{s1} &= z_{s1} \\ Z_{s2} &= \frac{z_{s2}^2 + z_{s1}z_{s2} - z_{t2}^2}{z_{s1} + z_{s2}}. \end{aligned} \tag{6}$$

V. Relation Between the Internal and External Impedance of Uncoated Distribution Cables

Uncoated cables practically act as grounding electrodes and, considering their usual lengths, they have very significant grounding effects. It has been shown in [23] that, at power frequency, the grounding effects of the uncoated metal-sheathed power cables, especially with steel armor, depend on the sheath internal impedance. To check the trend at higher frequencies, the following simple analysis of a single straight cable was considered.

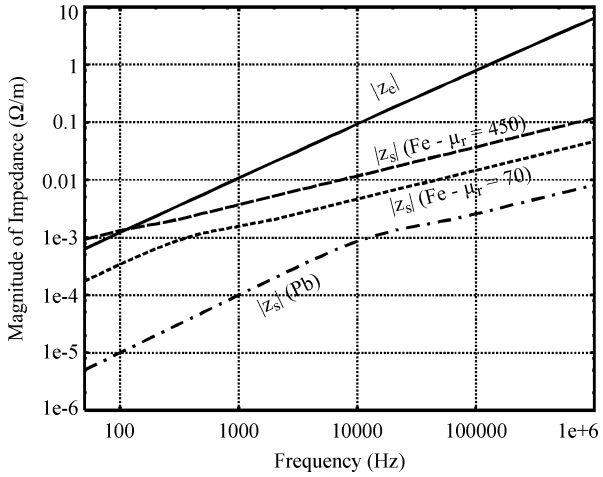

Fig. 4. Components of the impedance per unit length of steel-armored lead-sheathed cable.

A single straight cable may be analyzed using the transmission line techniques; see, for example, [30]. The propagation constant γ and characteristic impedance Z_c are given by

$$\begin{aligned} \gamma &= \sqrt{zy} \\ Z_c &= \sqrt{\frac{z}{y}} \end{aligned} \tag{7}$$

where z and y are the series impedance per unit length and the shunt admittance per unit length, respectively. Cable impedance to the ground may be determined as an input impedance of the open-circuited transmission line

$$Z_i = Z_c \coth \gamma\ell \tag{8}$$

where ℓ is the cable length.

The analysis of the significance of different parameters follows [30]. The impedance per unit length z is comprised of the earth (external) impedance z_e and cable surface (internal) impedance z_s:

$$z = z_e + z_s \tag{9}$$

and the admittance per unit length y is related to z_e [30] as

$$\begin{aligned} y &\approx \frac{\gamma_e^2}{z_e} \\ \gamma_e &= \sqrt{j\omega\mu_0(\sigma_e + j\omega\varepsilon_e)} \end{aligned} \tag{10}$$

It is of interest to compare z_s and z_e [see (9)].

Fig. 4 illustrates the comparison between the components of the impedance per unit length of typical steel-armored lead-sheathed cable in the frequency domain. The considered 10-kV cable with a 5-cm diameter has a 2-mm-thick lead sheath and

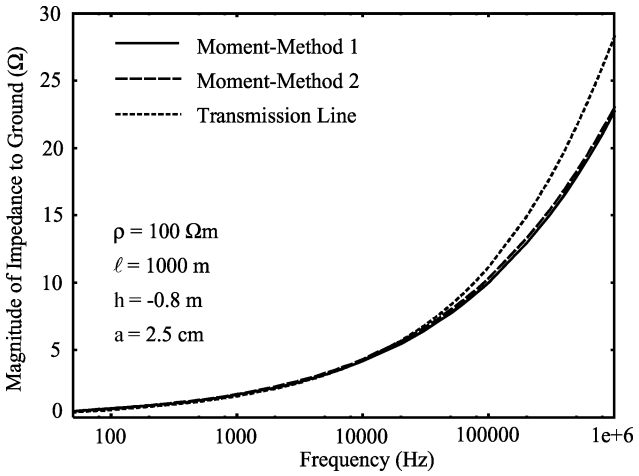

Fig. 5. Comparison of electromagnetic field theory and transmission line approaches. (Transmission line [32]. Moment method 1—piecewise sinusiodal Galekin's method [16]. Moment method 2—pulse expansion for currents and point matching [18]).

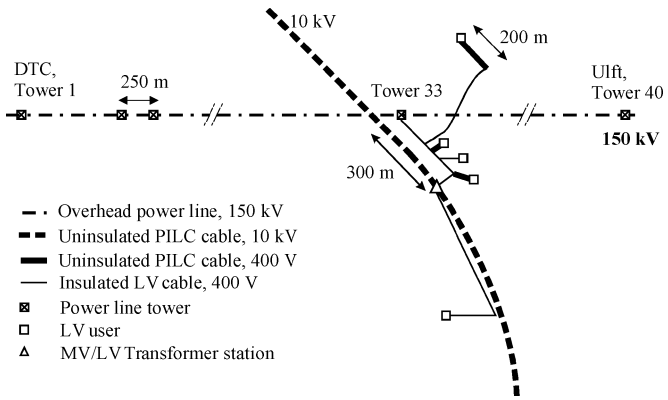

Fig. 6. Overview of the situation of the HV line and the LV/MV cable network. (Tower 33 is with the radio base-station system).

total of 1-mm steel tapes over the lead sheath in direct contact with the soil. We considered unsaturated steel (μ_r =450) when the current in the armor is about 400 A and saturated steel (μ_r =70) when the current in the armor is about 3 kA [31].

The values at the lowest frequencies of the internal impedance component of the armor are similar to (for unsaturated steel) or lower than (for saturated steel) the earth impedance, while they become much lower for higher frequencies. The results in Fig. 4 imply that the earth impedance component dominates over internal impedance especially at higher frequencies, except at the lowest frequencies. With this in mind, it is clear that evaluation of the earth impedance component is crucial for the modeling of uncoated cables at high frequencies.

VI. Comparison Between Electromagnetic and Transmission Line Approaches for Computation of the External Impedance of a Single Straight Cable

Fig. 5 gives a comparison of the computation results of the earth (external) impedance in a simple case of a straight single cable, using electromagnetic field theory and transmission line theory approaches. We considered a ℓ = 1000-m cable with $2a$ = 5-cm diameter buried in a depth of h = 0.8 m in ρ = 100-Ωm resistive soil. The impedance to the ground is computed by three approaches. One was based on the transmission line theory and the other on electromagnetic field theory. For the transmission line approach, we used techniques described in the well-known reference book of Sunde [32]. The propagation constant and characteristic impedance (7) were first evaluated following the methods in [32, ch. 5.4] and then the impedance to the ground (8) was computed.

For the electromagnetic field theory approach, we used two different techniques based on the method of moments described in [18]. One was the piecewise sinusoidal Galerkin method [16], while the other used pulse expansion functions for currents and point matching [18]. First, the current distribution was computed along the cable for a harmonic 1-A current injected at one end, then the voltage between the injection point and a reference point in the ground was computed by integrating the electric field vector along a path perpendicular to the cable. Impedance to the ground can be determined as a ratio between the voltage and injected current (4).

From the results in Fig. 5, it is evident that the electromagnetic and transmission line approaches are in excellent agreement at lower frequencies. Even in the higher part of the frequency range of interest the differences are not large, which can be expected for the symmetrical case of a long straight horizontal wire [33]. However, for complex geometries, it has been shown that differences become significant [34].

VII. Description of the Modeled Practical Case

A practical case of a radio base-station system mounted on the HV line tower, which is powered by an LV cable, was considered [5], [9], [10]. Fig. 6 gives an overview of the geometry.

The measurements were carried out on the 10.3-km-long double-circuit 150-kV link between the substations Doetinchem (DTC) and Ulft in the province Gelderland, which is served by the NUON power distribution company in the area. At a distance of 8.3 km from the DTC, tower 33 carries a radio base station. In the substation Ulft, tower 40 is directly connected to the local grounding grid. Two steel-reinforced aluminum conductor (ACSR) sky wires interconnect all towers. A 10-kV/400-V TS at about 300 m from tower 33 feeds the radio base station. The LV cross-linked polyethylene (XLPE) insulated cable toward the radio base station also feeds several customers; two other LV cables serve further customers. Some of the LV cables and the MV 10-kV cable are PILC cables. Their metallic shields are in good contact with the soil, and they are practically uncoated (or bare) and act as grounding electrodes. All cable shields at 10-kV/400-V TS are connected with the grounding system of the TS of about 3-Ω resistance to the ground. Therefore, all connected grounding systems and cable metallic shields act as a spatially extended grounding electrode arrangement. Fig. 7 illustrates the protection applied to the telecommunication cabinet at the base of tower 33. An insulating transformer in the cabinet separates HV and MV/LV systems. A varistor protects the insulating transformer and, when it is conductive, it connects the LV cable metallic shield and the tower grounding. It should be noted that this is one of the possible options for protection schemes considered in [3]

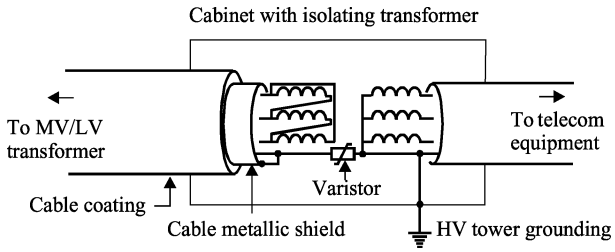

Fig. 7. Insulating transformer that insulates HV and MV/LV systems.

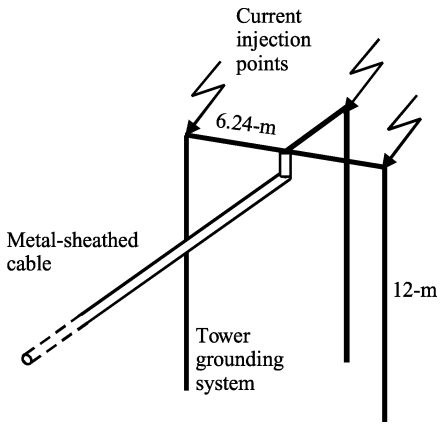

Fig. 8. Simplified model of the tower-33 grounding system and the connected cable shield.

and has been applied since January 1, 2000, in The Netherlands [35].

During the measurements at 50 Hz [5], [10], current was injected at the tower through a phase conductor from Doetinchem (DTC in Fig. 6). Taking into account the reduction factor of the sky wires, measurements indicate that, when the LV cable metallic shield is connected to the tower grounding, about 60% of the current injected at the top of tower 33 is carried to earth by the sky wires, and the rest descends down the tower and discharges to the earth through the tower grounding and the connected shields of the MV/LV cable network. Here, most of the current is led through the shields of the cable network and less than 10% reaches the ground through the tower grounding system.

VIII. Description of Adopted Models

A. Grounding System

The grounding system of tower 33 consists of three 12-m copper rods 2.5 cm in diameter. The actual value of the average soil resistivity was 100 Ωm, but an additional value of 1000 Ωm was also assumed for the simulation. In both cases, the relative permittivity of 10 was assumed. Fig. 8 illustrates the simplified model of the grounding system and the connection to the cable network. The grounding of the telecom equipment and the tower foundations, which are inside the area of the three rods, were ignored in this analysis.

B. Cable Network

Fig. 9 illustrates the layout of the simplified model of the LV/MV cable network used in the simulations. The cable shields

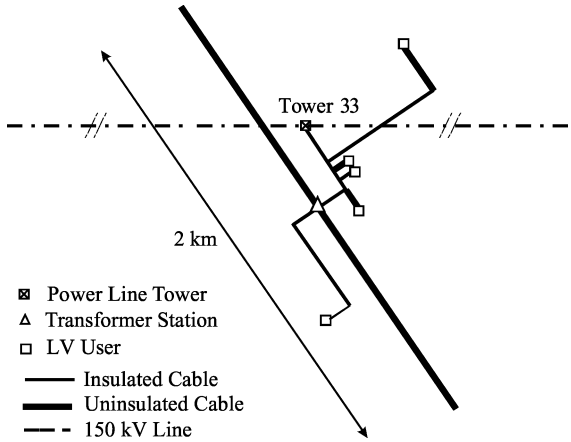

Fig. 9. Layout of the simplified model of the LV/MV cable network.

are directly connected to the grounding system. Therefore, it is assumed that the overvoltage arrestor acts as if it is short-circuited. The whole MV (10-kV) and part of the LV voltage cables are PILC, i.e., they have metal shields with good contact to the soil over their full length. Such cables act as grounding electrodes. Part of the LV XLPE insulated cables connects different grounding systems by means of their metal sheaths, so the whole structure is galvanically connected. The length of the PILC 10-kV cable was limited to 2 km in the calculations. The segmentation of the conductor network was nonhomogenous with a length of 30 cm at the tower, which gradually increased up to 20 m at the end of the 10-kV cable.

C. Sky Wires

The sky wires and towers with their groundings form a ladder network that may be considered as a series of Π circuits, allowing distributed parameter circuit theory to be approximately applied [26]. For completeness, details of the computational model are given in the Appendix.

Resistance per unit length of actual ACSR sky wires of 0.35 Ω/km was assumed, but as an alternative a value of 4.3 Ω/km, which is typical for steel sky wires, was also considered. The actual tower grounding low-frequency resistance to the ground of 3.5 Ω (in soil with a resistivity of 100 Ωm) was assumed. Correspondingly, a value of 35 Ω was assumed in the case of a soil resistivity of 1000 Ωm. Frequency-dependent impedance to the ground of the tower groundings was computed by the method described in Section III. As a first approximation, the tower was modeled with an inductance of 20 μH [36], [37].

IX. Computed Harmonic Impedances to Ground

A. Grounding System

All results in this section are for the actual case with a soil conductivity of 100 Ωm. Fig. 10 (solid line) shows the magnitude of the harmonic (frequency-dependent) impedance to the ground of the tower-33 grounding system alone, that is, when the cable shields are detached. At low frequency, the simulated value is in agreement with the measured value of 3.3 Ω [5], [10]. The behavior of the impedance at higher frequencies is typical:

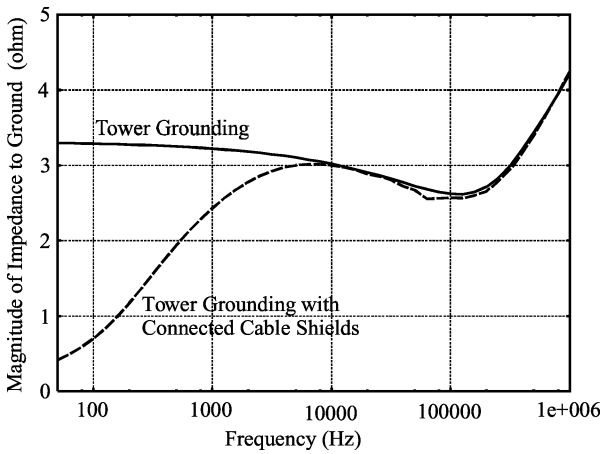

Fig. 10. Impedance to the ground of the tower grounding alone and with connected metal shields of MV/LV cables.

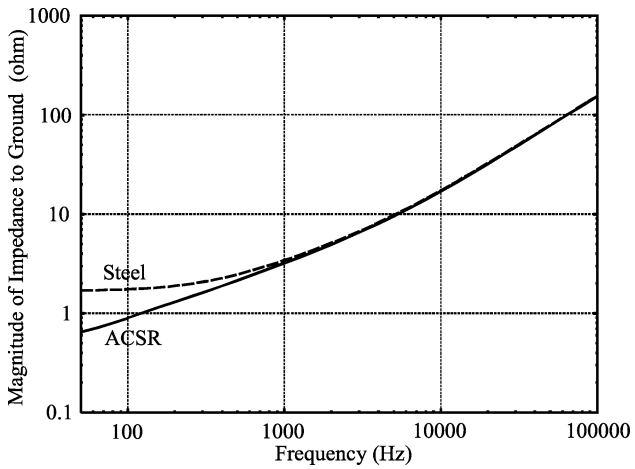

Fig. 11. Impedance to the ground of the sky wires.

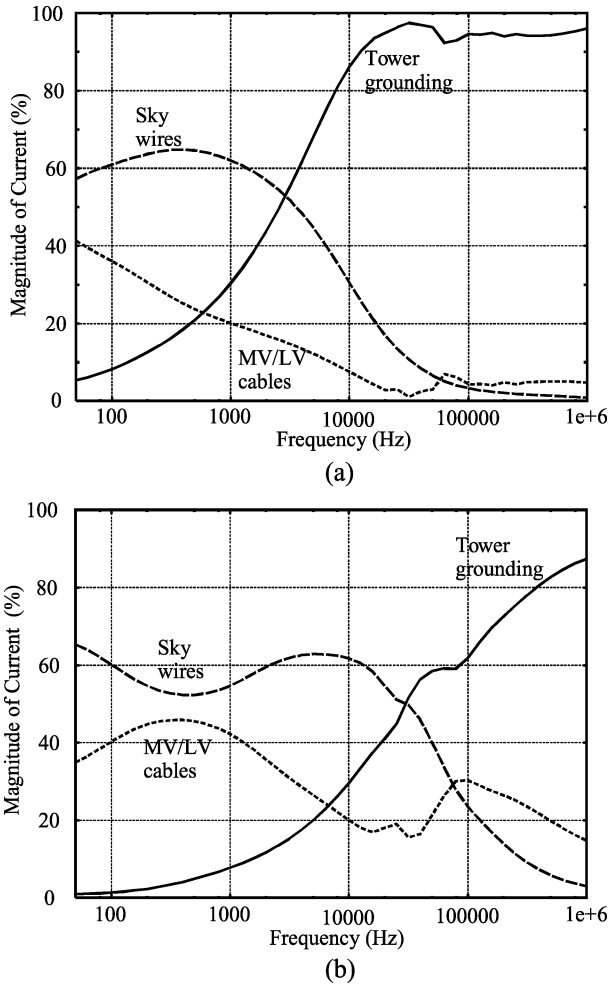

Fig. 12. Total current distribution between sky wires, tower grounding, and metal shields of MV/LV cables. (a) Soil $\rho = 100$ Ωm. (b) Soil $\rho = 1000$ Ωm.

after a slight decrease, it becomes dominantly inductive and increases above 100 kHz.

B. Grounding System With Connected Cable Shields

Fig. 10 (broken line) also shows the computed magnitude of the impedance to the ground of the grounding system and connected shields of the network of coated and uncoated cables. The value of the impedance to the ground is low at 50 Hz, where it is dominated by the influence of the cable network, which is in agreement with measurements, i.e., 0.4 Ω. However, it is very frequency-dependent and, at frequencies above 10 kHz, the influence of the cable shields diminishes, and the impedance to ground is totally dominated by the tower grounding system.

It is worth noting that the tower grounding system and the shields of the MV/LV cables are strongly coupled at higher frequencies; the coupling also depends on how the conductors are connected. This also justifies the 3-D electromagnetic analysis for the below-ground structures applied in this paper.

C. Sky Wires

Fig. 11 gives the impedance to the ground of the sky wires up to 100 kHz. The frequency dependence of the grounding effects of both steel and ACSR sky wires is dominated by the self-impedance of the wires. This also implies that a more precise modeling of towers and their groundings would not influence the impedance to the ground of sky wires at higher frequencies.

The impedance to the ground increases rapidly with frequency, much faster than the impedances to the ground of the grounding system and the cables. At 100 kHz, the difference is almost two orders of magnitude. This also justifies neglecting the mutual influences of the above- and below-ground structures in the modeling at high frequencies, implying that there is no coupling between them at high frequencies to the extent that it may be significant for the results.

X. Current-to-Ground Distribution: Frequency Domain

Current distribution between the sky wires and the grounding system connected to the cable network is first computed for current injected at the top of the tower. Results for lightning striking the tower are given in Fig. 12(a) for soil resistivity 100 Ωm.

At low frequencies, about 60% of the total current is distributed to the ground through the sky wires, about one third through shields of the connected network of MV/LV cables, and only a small part through the tower grounding, which is in agreement with the measurements [5], [10]. However, the situation

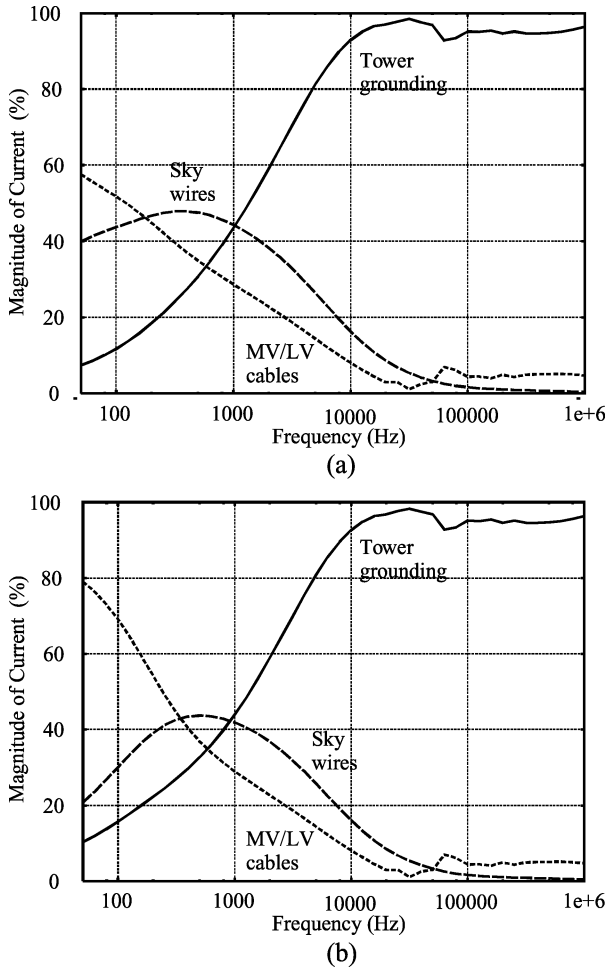

Fig. 13. Total current distribution between sky wires, tower grounding, and metal shields of MV/LV cables for lightning striking the sky wires near the tower. (a) ACSR sky-wire conductors. (b) Steel sky-wire conductors.

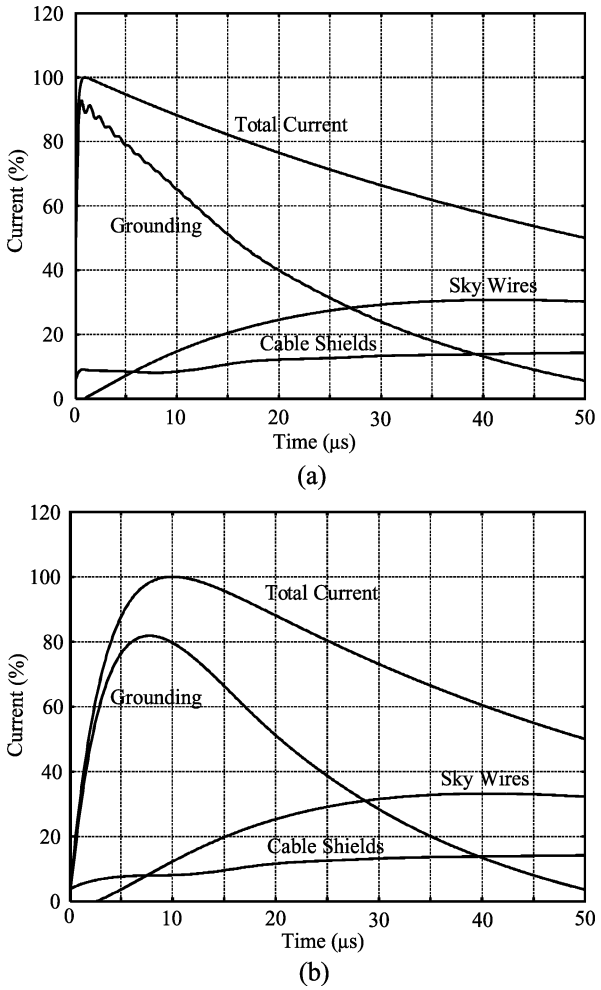

Fig. 14. Current distribution between the sky wires, the grounding, and the cable shields. Resistivity of soil $\rho = 100\ \Omega$m. (a) $T_1/T_2 = 1/50\ \mu s/\mu s$. (b) $T_1/T_2 = 10/50\ \mu s/\mu s$.

is changed in the kilohertz range, where above approximately 50 kHz nearly all current is guided to the ground through the tower-grounding system. The current distribution between the tower grounding system and the shields of the connected network of MV/LV cables is very frequency-dependent. With the rising frequency, the partial currents through cable shields diminish rapidly. Similarly, the part through the sky wires diminishes, but more slowly, leaving nearly all current (more than 90%) through the tower-grounding system above about 30 kHz.

Results for less conductive soil, with resistivity 1000 Ωm, are given in Fig. 12(b). The current distribution is not much different at 50 Hz compared to Fig. 12(a). However, at higher frequencies, the performance of the tower grounding is significantly decreased, leaving more current conducted through both sky wires and the cable network.

The influence of the lightning's location is illustrated in Fig. 13. In Fig. 13(a), the case similar to Fig. 12(a) with ACSR sky wires is computed except that the lightning strikes the sky wires near the tower. In this case, the direction of the current is different from that illustrated in Fig. 1, since the lightning current flows to the tower through sky wires and only one side of the sky wires conduct the current to the ground. The sky wires total impedance to ground $Z_{\rm sw}$ (Fig. 2) is about two times larger, and, consequently, their performance is decreased leaving more current in the sheaths of the cable network, especially at low frequencies.

Fig. 13(b) illustrates the influence of the conductivity of the sky wires when steel conductors are assumed. Less conductive sky wires (constructed of steel instead of ACSR) further decrease their grounding performance, leaving nearly 80% of the current in the sheaths of the cable network at 50 Hz.

It is clear that, in the case of lines without sky wires, even more current will be conducted through cable shields, especially at low frequencies.

XI. Current-to-Ground Distribution: Time Domain

Figs. 14 and 15 give the results for the lightning current distribution in the time domain for the same cases as in Fig. 12(a) and (b), respectively. Fig. 14 shows results for soil resistance of 100 Ωm and Fig. 15 for soil resistance of 1000 Ωm. Two different "double-exponential" current wave shapes [38] were considered: $T_1/T_2 = 1\ \mu$s/50 μs [in Figs. 14(a) and 15(a)] and $T_1/T_2 = 10\ \mu$s/50 μs [in Figs. 14(b) and 15(b)]. It should be noted that the small oscillations in the numerical results of the grounding current in Figs. 14(a) and 15(a) are due to the 1-MHz

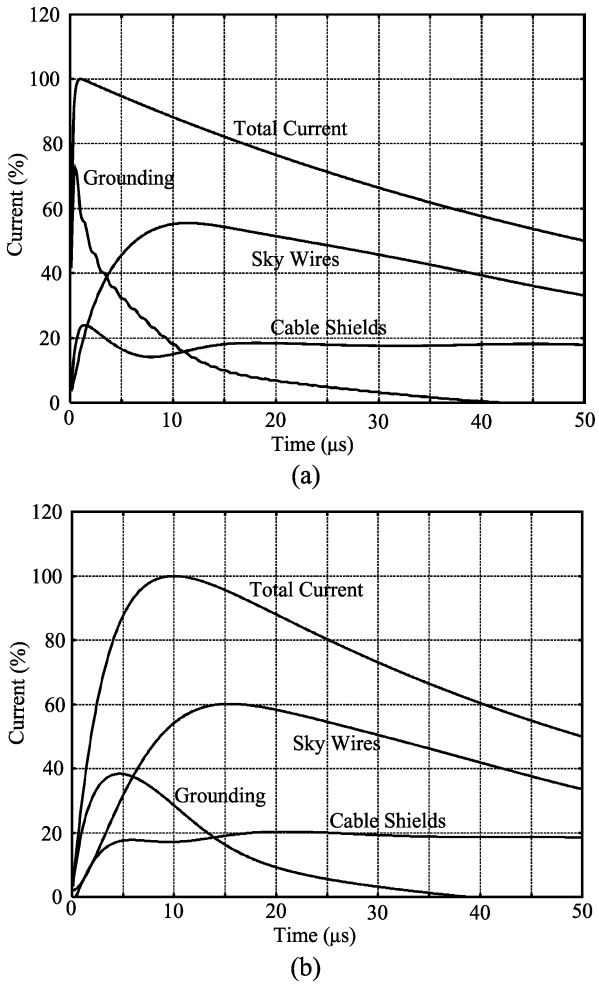

Fig. 15. Current distribution between the sky wires, the grounding, and the cable shields. Resistivity of soil $\rho = 1000\ \Omega$m. (a) $T_1/T_2 = 1/50\ \mu s/\mu s$. (b) $T_1/T_2 = 10/50\ \mu s/\mu s$.

upper frequency limit applied in the discrete Fourier transform; these would disappear if a higher frequency limit was applied.

The first conclusion from the results in Figs. 14 and 15 is that the performance of the grounding of the tower with the radio base station is very important in the first period after lightning strikes, when the most of the lightning current is discharged to the ground through it. After a few dozen microseconds (for the analyzed impulses), the tower grounding performance becomes nearly negligible compared to sky wires, which take about two thirds, and the cable network, which takes about one third of the total current. It should again be noted that this distribution is in agreement with measurements at 50 Hz.

The tower grounding takes more current in the first period when the lightning strikes for impulses with faster rise times [Figs. 14(a) and 15(a)] and for better conductive soil (Fig. 14). Also, its high performance lasts longer for better conductive soil. The importance of sky wires during the first part of the transient period is larger in less conductive soil (Fig. 15) and does not depend on the impulse wave shape.

These conclusions are consistent with the experimental study [39], [41] where horizontal counterpoises carried the bulk of the total lightning current away from the striking point, while ground rods near the striking point performed better for higher frequency components in the current.

The most important conclusion considers the grounding performance of the cable shields, which carried a limited and nearly constant part of the lightning current for all analyzed parameters. This is essential information in the practical analysis of the choice of the overvoltage arrestor.

It should be emphasized that results and conclusions are related to the specific case modeled. Other configurations of the cables and grounding systems may change the current distribution. Nevertheless, the models developed are general enough for estimation of the current distribution in other practical configurations.

XII. Conclusion

The paper describes a computer model for high frequencies and transients related to lightning in a network of buried conductors, consisting of grounding electrodes and uncoated and coated metallic shielded distribution cables. This model was applied to simulate the lightning current distribution to the ground in coupled HV and MV/LV systems.

The presented analysis was applied to one specific practical case, where a metal-shielded LV cable powered the radio base station on the HV tower. The case was considered when the ends of the LV cable shield were bonded to the HV tower grounding and to the LV/MV transformer station grounding. In turn, the LV/MV TS grounding system was connected to a network of coated and uncoated metal-shielded cables, acting as a spacious grounding system. For this case, the influence was investigated of parameters, such as the soil resistivity, quality of sky wires conductors, and location of the lightning strike. The following conclusions can be drawn.

- The grounding system of the tower with a radio base station is very important in the first part of the transient processes during the direct lightning strike. It discharges nearly all of the lightning current in the first moments, but, after dozens of microseconds, its performance reduces to nearly nothing compared to the sky wires and the metal shields of the cable network.
- High-quality sky wires are very important for discharging most of the lightning current to the ground after the first part of the transient processes. Moreover, in low conductive soil, their performance is dominant after the first few microseconds.
- Metallic cable shields take a limited, nearly time-independent, part of the lightning current. This part of the lightning current is larger in less conductive soil and with less conductive sky wires, for example, steel ones. Also, such current is larger for a strike on the sky wires compared to a strike at the tower.
- Nonlinearity of the tower grounding for high lightning currents improves its performance, particularly in low-resistive soil, which reduces the estimated current in the cable shields. Therefore, this model, which neglects this effect, overestimates the current in the cables (by a few

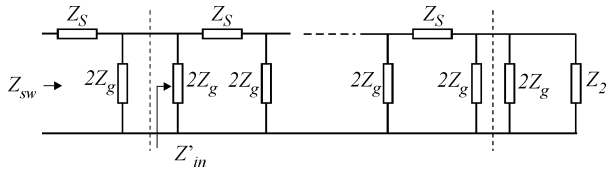

Fig. 16. Ladder network formed by the sky wires and towers with their groundings.

percent in the analyzed cases). In view of all other necessary assumptions, this might be considered as an approximation on the "safe" side.

Appendix
Parameters of the Ladder Network Formed by Sky Wires and Towers

The impedance to the ground at the sky wire connection to the tower $Z_{\rm sw}$ is equal to the input impedance of the distributed parameter circuit in Fig. 16 and is equal to [26]

$$Z_{\rm sw} = Z_s + \frac{2Z_g Z'_{\rm in}}{2Z_g + Z'_{\rm in}}$$
$$Z'_{\rm in} = Z_c \frac{\cosh(ng) + \frac{Z_c}{Z'_2}\sinh(ng)}{\sinh(ng) + \frac{Z_c}{Z'_2}\cosh(ng)}$$
$$Z'_2 = \frac{2Z_s Z_2}{2Z_s + Z_2}. \tag{A1}$$

Here g is the propagation constant, and Z_c is the characteristic impedance

$$g = \ln\left[1 + \frac{Z_s}{2Z_g} + \sqrt{\frac{Z_s}{Z_g} + \left(\frac{Z_s}{2Z_g}\right)^2}\right]$$
$$Z_c = \sqrt{\frac{Z_s \cdot 2Z_g}{2 + \frac{Z_s}{2Z_g}}}. \tag{A2}$$

Z_s is the impedance of the sky wires along a span, Z_g is the inductance of the tower and the impedance to ground of the tower grounding, Z_2 is the impedance to the ground connected to the sky wires at the end of the line, and n is the number of spans. The impedance of the sky wires along a span is equal to

$$Z_s = z_{\rm sw} \cdot \ell. \tag{A3}$$

The term ℓ is the length of the span, and $z_{\rm sw}$ is the impedance per unit length of the sky wires considered as conductors with earth return. $z_{\rm sw}$ was computed using the program "LINE CONSTANTS" [40] of the ATP version of EMTP [4].

References

[1] *IEEE Guide for Improving the Lightning Performance of Transmission Lines*, IEEE Stand. 1243-1997, Dec. 1997.

[2] W. A. Chisholm, S. L. Cress, and J. Polak, "Lightning-caused distribution outages," in *Proc. IEEE Power Eng. Soc. Transmission Distribution Conf.*, 2001, pp. 1041–1046.

[3] Protection Measures for Radio Base Stations Sited on Power Line Towers. ITU-T Recommendation K.57. Available. [Online] http://www.itu.int

[4] H. W. Dommel, *Electromagnetic Transients Program. Reference Manual (EMTP Theory Book)*. Portland, OR: Bonneville Power, 1986.

[5] J. B. M. van Waes, "Safety and EMC aspects of grounding," Ph.D. dissertation, Eindhoven Univ. of Technol., Eindhoven, The Netherlands, Oct. 2003.

[6] H. Zeuschel and P. Hoiss, "Low voltage supplied to mobile base stations on high voltage tower," *EVU-Betriebspraxis*, vol. 37, pp. 8–11, Dec. 1998.

[7] E. Montandon, "Mobile telephone antennas on high voltage power line masts," in *Proc Int. Conf. Lightning Protection*, Cracow, Poland, 2002, pp. 728–731.

[8] G. Balzer, O. Schmitt, and B. Richter, "Protection of mobile phone stations in high voltage towers against over voltages generated by lightning," in *Proc. 26th Int. Conf. Lightning Protection*, Cracow, Poland, 2002, pp. 785–788.

[9] J. B. M. van Waes, A. P. J. van Deursen, P. C. T. van der Laan, M. J. M. van Riet, F. Provoost, and J. F. G. Gobben, "Risks due to lightning strikes on high voltage towers with LV applications," in *Proc. 25th Int. Conf. Lightning Protection*, Rhodes, Greece, 2000, pp. 837–841.

[10] J. B. M. van Waes, A. P. J. van Deursen, M. J. M. van Riet, and F. Provoost, "Safety aspects of GSM systems in high-voltage towers: an experimental analysis," *IEEE Trans. Power Del.*, vol. 17, no. , pp. 550–554, Apr. 2002.

[11] Y. Rajotte, J. Fortin, and G. Raymond, "Impedance of multigrounded neutrals on rural distribution systems," *IEEE Trans. Power Del.*, vol. 10, pp. 1453–1459, Jul. 1995.

[12] C. T. Mata, M. I. Fernandez, V. A. Rakov, and M. A. Uman, "EMTP modeling of a triggered-lightning strike to the phase conductor of an overhead distribution line," *IEEE Trans. Power Del.*, vol. 15, pp. 1175–1181, Oct. 2000.

[13] E. Petrache, M. Paolone, F. Rachidi, C. A. Nucci, V. Rakov, M. Uman, D. Jordan, K. Rambo, M. Nyffeler, J. Schoene, A. Cordier, and T. Verhaege, "Measurement of lightning-induced currents in an experimental coaxial buried cable," in *Proc. IEEE PES General Meeting*, vol. 1, Toronto, ON, Canada, 2003, pp. 262–267.

[14] F. M. Tesche, B. A. Renz, R. M. Hayes, and R. G. Olsen, "Development and use of a multiconductor line model for PLC assessments," in *Proc. Int. Zurich Symp. Electromagn. Compat.*, 2003, pp. 99–104.

[15] R. G. Olsen and M. C. Willis, "A comparison of exact and quasistatic methods for evaluating grounding systems at high frequencies," *IEEE Trans. Power Del.*, vol. 11, pp. 1071–1081, Apr. 1996.

[16] L. Grcev, "Computer analysis of transient voltages in large grounding systems," *IEEE Trans. Power Del.*, vol. 11, pp. 815–823, Apr. 1996.

[17] J. H. Richmond, "Radiation and scattering by thin-wire structures in the complex frequency domain," in *Computational Electromagnetics*, E. K. Miller, L. Medgyesi-Mitschang, and E. H. Newman, Eds. New York: IEEE Press, 1992.

[18] L. Grcev, "Computation of transient voltages near complex grounding systems caused by lightning currents," in *Proc. IEEE Int. Symp. Electromagn. Compat.*, 1992, pp. 393–399.

[19] J. H. Richmond, "Computer Program for Thin-Wire Structures in a Homogeneous Conducting Medium," National Aeronautics and Space Admin., Washington, DC, Tech. Rep. TR 2902-10, May 1974.

[20] ASAP—A General Purpose User-Oriented Computer Program for Analysis of Thin-Wire Structures in the Presence of Finite Ground, J. W. McCormack and R. L. Cross. *http://home.att.net/~ray.l.cross/asap* [Online]

[21] L. Grcev and V. Filiposki, "Earth potential distribution around high voltage substations in rural and urban areas," in *Proc. Int. Zurich Symp. Electromagn. Compat.*, 1997, pp. 483–488.

[22] R. W. P. King, "Antennas in material media near boundaries with application to communication and geophysical exploration, part I: the bare metal dipole," *IEEE Trans. Antennas Propagat*, vol. AP-34, no. 4, pp. 483–489, Apr. 1986.

[23] J. Nahman and D. Salamon, "Effects of the metal sheathed cables upon the performances of the distribution substations grounding systems," *IEEE Trans. Power Del.*, vol. 7, pp. 1179–1187, Jul. 1992.

[24] J. Nahman, "Earthing effects of coated underground cables with metallic shields bonded to earth electrodes," *Proc. Inst. Elect. Eng.—Gener. Transm. Distribut.*, vol. 144, pp. 26–30, Jan. 1997.

[25] J. M. Nahman, J. B. Djordjevic, and D. Salamon, "Grounding effects of HV and MV underground cables associated with urban distribution substations," *IEEE Trans. Power Del.*, vol. 17, no. 1, pp. 111–116, Jan. 2002.

[26] J. Nahman, *Neutral Grounding in Distribution Networks* (in Serbian). Belgrade, Yugoslavia: Naucna Knjiga, 1980.
[27] J. H. Richmond and E. H. Newman, "Dielectric coated wire antennas," *Radio Sci.*, vol. 11, pp. 13–20, Jan. 1976.
[28] *Handbook of Mathematical Functions With Formulas, Graphs, and Mathematical Tables*, M. Abramowitz and I. A. Stegun, Eds., Dover, New York, 1965.
[29] A. Tsailovich, *Cable Shielding for Electromagnetic Compatibility*. New York: Van Nostrand Reinhold, 1995.
[30] E. F. Vance, *Coupling to Shielded Cables*. New York: Wiley, 1978.
[31] *Technical Handbook* (in Croatian), Koncar, Zagreb, Croatia, 1991.
[32] E. D. Sunde, *Earth Conduction Effects in Transmission Systems*. New York: Dover, 1968, ch. 5.4.
[33] C. R. Paul, *Analysis of Multiconductor Transmission Lines*. New York: Wiley, 1994.
[34] M. Heimbach and L. Grcev, "Simulation of grounding structures within EMTP," in *Proc. Int. Symp. High Voltage Eng.*, vol. 5, Montreal, QC, Canada, 1997, pp. 131–134.
[35] "GSM Antenna in HV Tower," (in Dutch), , Canada, NUON Directive N5590, 1999.
[36] A. F. Imece, D. W. Durbak, H. Elahi, S. Kolluri, A. Lux, D. Mader, T. E. McDermott, A. Morched, A. M. Mousa, R. Natarajan, L. Rugeles, and E. Tarasiewicz, "Modeling guidelines for fast front transients," *IEEE Trans. Power Del.*, vol. 11, no. 1, pp. 493–506, Jan. 1996.
[37] *Transmission Line Reference Book, 345 kV and Above*, 2nd ed. Palo Alto, CA: Electric Power Research Inst., 1982.
[38] C. Mazzetti and G. M. Veca, "Impulse behavior of ground electrodes," *IEEE Trans. Power App. Syst.*, vol. PAS-102, pp. 3148–3156, Sep. 1983.
[39] M. Bejleri, V. A. Rakov, M. A. Uman, K. J. Rambo, C. T. Mata, and M. I. Fernandez, "Triggered lightning testing of an airport runway lighting system," *IEEE Trans. Electromagn. Compat.*, vol. 46, pp. 96–101, Feb. 2004.
[40] *Alternative Transients Program (ATP) Rule Book*, Canadian/Amer. EMTP User Group, 1992.
[41] M. Bejleri, V. A. Rakov, M. A. Uman, K. J. Rambo, C. T. Mata, and M. I. Fernandez, "Triggered lightning testing of an airport runway lighting system," in *Proc. Int. Conf. Lightning Protection*, Rhodes, Greece, 2000, pp. 825–830.

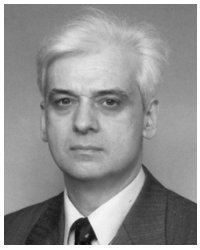

Leonid Grcev (M'84–SM'97) was born in Skopje, Macedonia in 1951. He received the Dipl.-Ing. from the Sts. Cyril and Methodius University, Skopje, Macedonia, in 1978 and the M.S. and Ph.D. degrees from the University of Zagreb, Zagreb, Croatia, in 1982 and 1986, respectively, all in electrical engineering.

From 1978 to 1988, he was with the Telecommunications Department, Electric Power Company of Macedonia. Since 1988, he has been a member of the Faculty of Electrical Engineering at the Sts. Cyril and Methodius University as an Assistant Professor, Associate Professor, and Vice Dean. He currently holds the position of Full Professor. He has been a Visiting Professor with the Technical University of Aachen, Aachen, Germany, the Swiss Federal Institute of Technology, Lausanne, and the Eindhoven University of Technology, Eindhoven, The Netherlands. He was responsible for several international projects related to electromagnetic compatibility (EMC). He is the author and coauthor of more than 100 scientific papers published in reviewed journals and presented at international conferences. His research interests concern power system EMC and modeling of grounding systems and connected structures at high frequencies and transients with particular reference to lightning.

Prof. Grcev is a member of the CIGRE and CIRED Working Groups related to EMC and lightning and has been a chairperson and a member of scientific committees in international conferences.

A. (Lex) P. J. van Deursen (SM'97) received the Ph.D. degree in physics from the Katholieke Universiteit, Nijmegen, The Netherlands, in 1976. His dissertation focused on an experimental study in molecular physics concerning weakly bound atomic and molecular complexes.

After a Postdoctoral position with the Max Planck Institut für Festkörperforschung, Hochfeld Magnetlabor, Grenoble, France, he returned to Nijmegen to work in solid-state physics on electronic structures of metals, alloys, and semiconductors using high magnetic field techniques. In 1986, he joined the Eindhoven University of Technology, Eindhoven, The Netherlands, and shifted his attention to electromagnetic compatibility.

Prof. van Deursen is a member of CIGRE SC36 and CENELEC. He has been engaged in several IEC working groups and has been chairman and member of different committees in international conferences.

J. B. M. van Waes was born in Breda, The Netherlands, in 1973. He received the M.Sc. degree in electrotechnical engineering and the Ph.D. degree from the Eindhoven University of Technology, Eindhoven, The Netherlands, in 1996 and 2003, respectively.

As an Associate Scientist, he worked on a multimedia course on electromagnetic compatibility (EMC) and on different projects related to grounding for industry with the Eindhoven University of Technology. In December 1997 he performed his doctoral work in cooperation with the Dutch Power Distribution Company NUON on various aspects of grounding in large utility grids. He is currently with the Holland Railconsult Company, Utrecht, The Netherlands.